

# Flow characteristics of natural circulation in a lead–bismuth eutectic loop

Chen-Chong Yue<sup>1,2</sup> · Liu-Li Chen<sup>2</sup> · Ke-Feng Lyu<sup>1,2</sup> · Yang Li<sup>2</sup> · Sheng Gao<sup>2</sup> · Yue-Jing Liu<sup>2</sup> · Qun-Ying Huang<sup>2</sup>

Received: 11 August 2015/Revised: 23 October 2015/Accepted: 17 November 2015/Published online: 11 February 2017  
© Shanghai Institute of Applied Physics, Chinese Academy of Sciences, Chinese Nuclear Society, Science Press China and Springer Science+Business Media Singapore 2017

**Abstract** Lead and lead-alloys are proposed in future advanced nuclear system as coolant and spallation target. To test the natural circulation and gas-lift and obtain thermal-hydraulics data for computational fluid dynamics (CFD) and system code validation, a lead–bismuth eutectic rectangular loop, the KYLIN-II Thermal Hydraulic natural circulation test loop, has been designed and constructed by the FDS team. In this paper, theoretical analysis on natural circulation thermal-hydraulic performance is described and the steady-state natural circulation experiment is performed. The results indicated that the natural circulation capability depends on the loop resistance and the temperature and center height differences between the hot and cold legs. The theoretical analysis results agree well with, while the CFD deviate from, the experimental results.

**Keywords** Accelerator-driven systems · Lead–bismuth eutectic · Natural circulation · CFD

## 1 Introduction

Due to their chemical inertness and good thermal-physical properties, which are in favor of the reactors' reliability and safety, liquid lead or lead–bismuth eutectic (LBE) were proposed as a potential candidate coolant material for future advanced nuclear systems such as accelerator-driven systems (ADS) and lead-cooled fast reactors (LFR) [1]. The high atomic number of LBE makes it also suitable as a spallation target of ADS which has been proposed for the transmutation of nuclear waste [2, 3].

Owing to the property of large thermal expansion coefficient, a significant natural circulation capability emerges in HLM (heavy liquid metal)-cooled reactor designs [4]. Natural circulation is driven by the hydrostatic head due to the density difference of LBE between the hot and cold legs. It takes away the heat generated in the reactor core via natural circulation of the coolant under accident conditions. Natural circulation even has been adopted as the normal operation mode for primary cooling in some advanced HLM-cooled reactor designs, e.g., the small secure transportable autonomous reactor (SSTAR) [5, 6], one of the generation-IV designs proposed in the USA. As the passive safety and reliability is likely being employed for generation-IV nuclear reactors, attentions have been increasingly given to natural circulation performance in the advanced reactor designs.

Both theoretical and experimental efforts were made to study natural circulation of LBE in various nuclear reactor systems. Davis analyzed thermal-hydraulics of HLM-cooled reactors [7]. Ma et al. [8, 9] did experiments on forced flow and natural circulation of LBE, and its stability, for ADS in TALL facility. Tarantino et al. [10] carried out steady-state pretest analysis of an LBE test loop, NACIE,

---

This work was supported by the National Natural Science Foundations of China (Nos. 51401205 and 51301163) and the Strategic Priority Research Program of Chinese Academy of Sciences (No. XDA03040000).

---

✉ Liu-Li Chen  
liuli.chen@fds.org.cn

<sup>1</sup> School of Nuclear Science and Technology, University of Science and Technology of China, Hefei 230027, China

<sup>2</sup> Key Laboratory of Neutronics and Radiation Safety, Institute of Nuclear Energy Safety Technology, Chinese Academy of Sciences, Hefei 230031, China

through steady-state 1D analysis and 3D CFD studies. Borgohain et al. [11] investigated natural circulation in HANS test loop and indicated that natural circulation capability depended on loop structure parameters.

An engineering project to develop ADS and lead-based fast reactors technology was launched in China in 2011, with the CLEAR (China lead-based reactor) being the reference reactor for ADS and fast reactor. It is performed by a number of institutions led by Institute of Nuclear Energy Safety Technology, Chinese Academy of Sciences (INEST). To support the design and construction of CLEAR-I, an LBE rectangular loop named KYLIN-II Thermal Hydraulic (KYLIN-II TH) natural circulation test loop was constructed on the basis of available experience on lead–lithium technology [12], including the fusion reactor design [13–15], R&D on blanket [16, 17], R&D on fusion materials and technologies [18–20]. To verify the capability of natural circulation in KYLIN-II TH natural circulation test loop, it is necessary to analyze flow characteristics of natural circulation. One of the goals of KYLIN-II facility is to carry out natural circulation experiments under different conditions, aiming at, among others, supporting the verification and validation of numerical codes.

In this paper, steady-state experiments on natural circulation with different heating powers are performed in the loop. The results are compared with theoretical analysis and CFD simulation results.

## 2 KYLIN-II TH natural circulation loop

The KYLIN-II TH natural circulation loop is an LBE rectangular loop as depicted in Fig. 1. The loop basically consists of two vertical pipes working as riser and

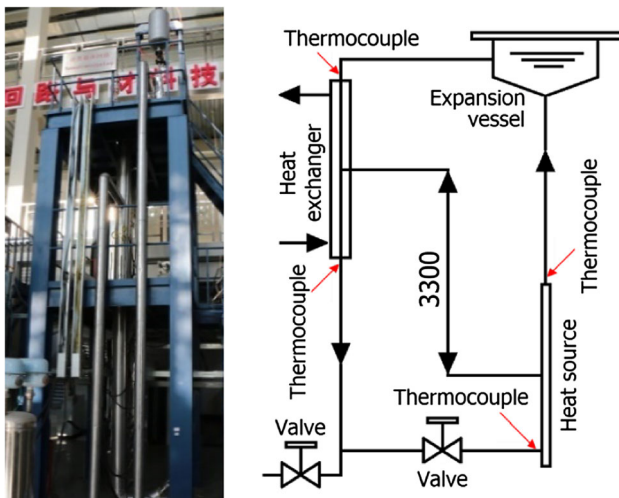


**Fig. 1** Layout of the KYLIN-II TH natural circulation loop

downcomer, respectively, connected by two horizontal branches. In the bottom part of the riser, a heat source (HS) of 24.0 kW is installed, while the upper part of the downcomer is connected to a heat exchanger (HX). An expansion vessel is installed on the loop top, coaxially to the riser. By a valve installed in the cold part of the loop, the singular pressure losses of the system are modified in the tests. Table 1 shows the main parameters of the loop.

The HS is arranged at the bottom of the riser containing an electrical rod simulator, which is concentrically inserted in a 54-mm-ID tube made of 316L stainless steel. The inner diameter of HS is larger than the main pipe of the loop, for the average velocity in the main pipe, it is estimated  $0.12\text{--}0.25\text{ m s}^{-1}$ , while, and it is about  $0.03\text{--}0.06\text{ m s}^{-1}$  for the velocity inside the HS. Connected coaxially to the top of the riser, the expansion vessel provides a suitable volume to allow the LBE expansion when it is heated to hundreds of degrees in the test. To avoid the LBE being oxidized, the free level of LBE is covered by argon gas with a slight overpressure of tens of kPa. Considering the heat exchange capability without introducing extra pressure loss, a ‘tube-in-tube,’ counter-flow-type heat exchanger is adopted. High-temperature heat-conducting oil is used as the secondary fluid. Four immersion K-type thermocouples are installed at the both ends of the HS and HX to measure the loop temperature.

## 3 Theoretical analysis

### 3.1 Theoretical analysis model for natural circulation

A one-dimensional theoretical model is adopted for analyzing natural circulation in the KYLIN-II TH natural circulation loop. For calculating the LBE flow rate through

**Table 1** Main parameters of the KYLIN-II TH natural circulation loop

Parameters	Values
Total height (m)	5
Length of HS (mm)	1800
Pipe inner diameter (mm)	26
HS inner diameter (mm)	54
Electrical rod diameter (mm)	22
Active heating length (mm)	800
Operating temperature (°C)	150–500
Operating pressure (atm)	1–1.5
Input power (kW)	0–24
Maximum wall heat flux ( $\text{W cm}^{-2}$ )	43.4

the loop, the momentum equation under steady-state condition, integrated along the whole loop, can be written as:

$$\Delta P_D = \Delta P_{fr}, \tag{1}$$

where  $\Delta P_D$  is the driving force for the natural circulation and  $\Delta P_{fr}$  the total friction along the loop.

The driving force is caused by density difference of LBE between the hot and cold legs and is related to the temperature difference (thermal buoyancy). According to the energy conservation law, the temperature difference can be calculated with the input power of the electrical rod simulator ( $P_{th}$ ), the specific heat capacity of the fluid ( $c_p$ ) and the mass flow rate of LBE ( $\dot{m}$ ). Thus, the driving force term can be written as:

$$\Delta P_D = \rho_0 \beta g H P_{th} / (\dot{m} c_p), \tag{2}$$

where  $\rho_0$  is the fluid density corresponding to the average temperature in the loop,  $\beta$  is the fluid isobaric thermal expansion coefficient,  $g$  is gravitational acceleration, and  $H$  is the effective elevation change between heating and cooling centers.

To evaluate the total pressure drop along the flow path, a total singular pressure drop coefficient is defined as:

$$K = \sum_i \left[ \left( k + f \frac{L}{D_H} \right) \frac{A_{pipe}^2}{A_i^2} \right], \tag{3}$$

where  $k$  is the singular pressure drop coefficient in the  $i$ th branch of the loop;  $f$  is the Darcy–Weisbach friction factor in the  $i$ th branch of the loop;  $L$ ,  $D_H$  and  $A_i$  are the length, hydraulic diameter and flow area of the  $i$ th branch of the loop, respectively; and  $A_{pipe}$  is the main cross section along the flow path. The total singular pressure drop coefficient is discussed again in Sect. 3.2.

The friction term in Eq. (1) can be expressed as:

$$\Delta P_{fr} = K \frac{1}{2} \rho_0 v^2 = \frac{1}{2} K \frac{\dot{m}^2}{\rho_0 A_{pipe}^2}, \tag{4}$$

where  $v$  is the velocity in main pipe.

Assuming that  $K$  does not depend on the velocity, and using Eqs. (1), (2) and (4), the mass flow rate in the natural circulation flow regime can be calculated by Eq. (5).

$$\dot{m} = \left( \frac{2\beta\rho_0^2 g H A_{pipe}^2 P_{th}}{c_p K} \right)^{\frac{1}{3}} \tag{5}$$

The  $\dot{m}$  and  $K$  can be optimized as a function of the Reynolds number. Finally, the results can be optimized by iteration.

### 3.2 Resistance coefficients of parts and components

The resistance coefficient of the loop in Eq. (3) can be obtained by a thermal-hydraulic modeling for different parts of the primary loop. The total singular pressure drop coefficient  $K$  can be expressed by:

$$K = K_{HS} + K_{EV} + K_{pipe}, \tag{6}$$

where  $K_{HS}$  is the pressure drop coefficient in HS;  $K_{EV}$  is the pressure drop coefficient in expansion vessel; and  $K_{pipe}$  is the pressure drop coefficient along the pipe. Since the cross section of the tube in HX is coincident with the cross section of the pipe,  $K_{pipe}$  contains the pressure drop in HX, and the pressure drop in two 90° elbows is included in  $K_{pipe}$ , too.

As the flow area in the HS differs from the pipe cross section, and the flow direction changes, the pressure drop coefficient in HS can be written as:

$$K_{HS} = K_{in} + K_{out} + K_{l,eff}, \tag{7}$$

where  $K_{in}$  is the pressure drop coefficient of the HS inlet, consisting of the effects of changes in flow direction (a T-shaped elbow with one end blocked,  $K = 1.29$ ) [21] and the flow area ( $K \approx 0.64$ );  $K_{out}$  is the pressure drop coefficient of the HS outlet, mainly influenced by the change in flow area; and  $K_{l,eff}$  is the pressure drop coefficient along the HS, defined as:

$$K_{l,eff} = \frac{f L_{HS}}{D_H} \left( \frac{A_{pipe}}{A_{HS}} \right)^2, \tag{8}$$

where  $f$  is the Darcy–Weisbach friction factor;  $L_{HS}$  is the HS length;  $D_H$  is hydraulic diameter of the HS; and  $A_{HS} = A - A_r$  is flow area of the HS, with  $A$  being the cross section of HS and  $A_r$ , cross section of the heater.

The pressure drop in expansion vessel is caused by the inlet ( $K \approx 1$ ), the outlet ( $K \approx 0.5$ ) and the change in flow direction, and some chemical control instrumentation ( $K \approx 1$ ) as well. According to previous experience on other loops of KYLIN-II facility, the resistance coefficient of the expansion vessel is  $K_{EV} \approx 2.5$ .

It is assumed conservatively that the total length of the pipe (I.D. = 26 mm) is  $L_{pipe} \approx 11$  m with 2°–90° elbows ( $K = 0.5 \times 2 = 1$ , the other two elbows for the expansion vessel and the HS, respectively) [21]. The resistance coefficient, for the pressure drop along the pipe and 2 (90°) elbows, can therefore be expressed as:

$$K_{pipe} = \frac{f L_{pipe}}{D} + 1. \tag{9}$$

### 3.3 The preliminary results of theoretical analysis

The thermal-hydraulic performance in natural circulation can be calculated with geometrical configuration of the loop known. According to the approaches in Sect. 3.2, the hydraulic parameters of Reynolds numbers, resistance coefficients and overall pressure loss can be calculated as a function of the LBE mass flow rate. The main results are listed in Table 2. The total singular pressure drop

coefficient declines with the mass flow rate, mainly because the  $K_{\text{pipe}}$  declines with increasing Reynolds number.

By solving Eq. (5), one can estimate the equilibrium mass flow rate of natural circulation in the loop at different input powers. The main thermal-hydraulic parameters at different power levels are summarized in Table 3.

## 4 The CFD simulation

### 4.1 Description of CFD modeling

CFD simulations were carried to evaluate the KYLIN-II natural circulation loop, together with the expansion tank. The geometry model of expansion tank, heating rod and HX was adopted as shown in Fig. 2. The valve at the bottom was replaced by a tube. The 3D geometry was modeled in ICEM CFD (the Integrated Computer Engineering and Manufacturing code for Computational Fluid Dynamics) with dimensions of the pipes and other key component described in Sect. 2. The heating volume did not consist of solid volume; only a surface source on the pin wall was adopted. A commercial code FLUNET was employed to simulate the steady state of natural circulation at different heating powers.

The simulation model is RNG  $\kappa$ - $\varepsilon$  model with standard wall treatment [11]. The heating powers of 4.3, 7.6, 11.2, 15.3 and 17.9 kW were decided on experimental basis. Correspondingly, the heat fluxes of 5.15, 9.20, 13.47, 18.40 and 21.52  $\text{W cm}^{-2}$  were imposed on the rod bundle surface. Regarding the HX, a heat transfer coefficient of 4.89  $\text{W cm}^{-2} \text{K}^{-1}$  and a free stream temperature of 200 °C were utilized on the oil side. After a sensitivity analysis on the unstructured mesh, the grid numbers were defined as  $1.3 \times 10^6$  °C.

### 4.2 CFD simulation results of the steady-state experiments

The CFD results at different input powers were obtained using FLUENT. The temperature and velocity contours at heating power of 17.9 kW are shown in Fig. 3. The

**Table 3** Thermal-hydraulic performance matrix in natural circulation

$P$ (kW)	$\dot{m}$ ( $\text{kg s}^{-1}$ )	$\Delta T$ (°C)	$v$ ( $\text{m s}^{-1}$ )
4	0.657	41.4	0.119
8	0.834	65.3	0.151
12	0.957	85.3	0.174
16	1.058	102.9	0.192
20	1.143	119.1	0.208
24	1.215	134.4	0.221

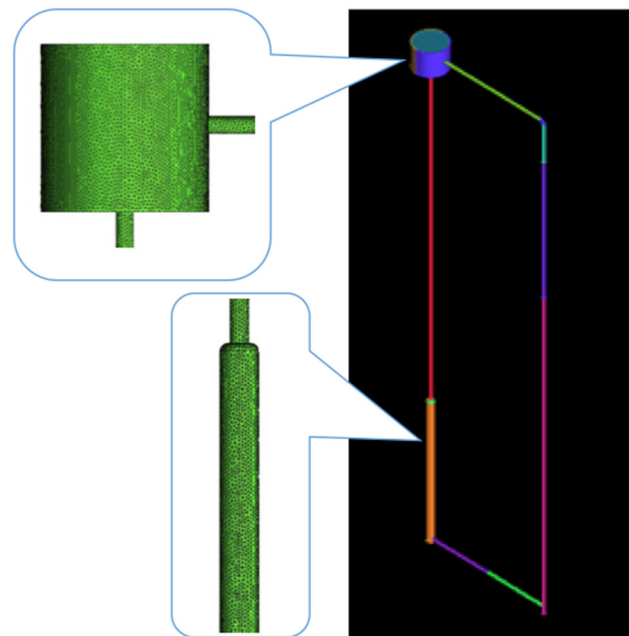


**Fig. 2** 3D geometry model and unstructured grid mesh of the loop

maximum temperature appeared on upper end of the heating rod (Fig. 3a). The loop was assumed adiabatic, without heat losses, so the outlet temperature of HX matches with the inlet temperature of HS. The HS outlet temperature was 334.4 °C, and the temperature difference through the HS was 101.5 °C. From Fig. 3b, the velocity through all pipes was almost constant, hence a steady state.

**Table 2** Reynolds numbers, resistance coefficients and overall pressure loss as a function of the LBE mass flow rate

$\dot{m}$ ( $\text{kg s}^{-1}$ )	$Re_{\text{tube}} (\times 10^3)$	$Re_{\text{HS}} (\times 10^3)$	$K_{\text{HS}}$	$K_{\text{EV}}$	$K_{\text{pipe}}$	$K_{\text{total}}$	$\Delta P_{\text{fr}}$ (Pa)
0.25	5.56	1.90	2.9	2.5	19.1	24.5	261.9
0.5	11.10	3.81	2.8	2.5	18.9	24.2	1034.8
0.75	16.70	5.71	2.8	2.5	18.5	23.8	2289.9
1	22.30	7.62	2.7	2.5	18.1	23.3	3985.4
1.25	27.80	9.52	2.6	2.5	17.7	22.8	6093.6

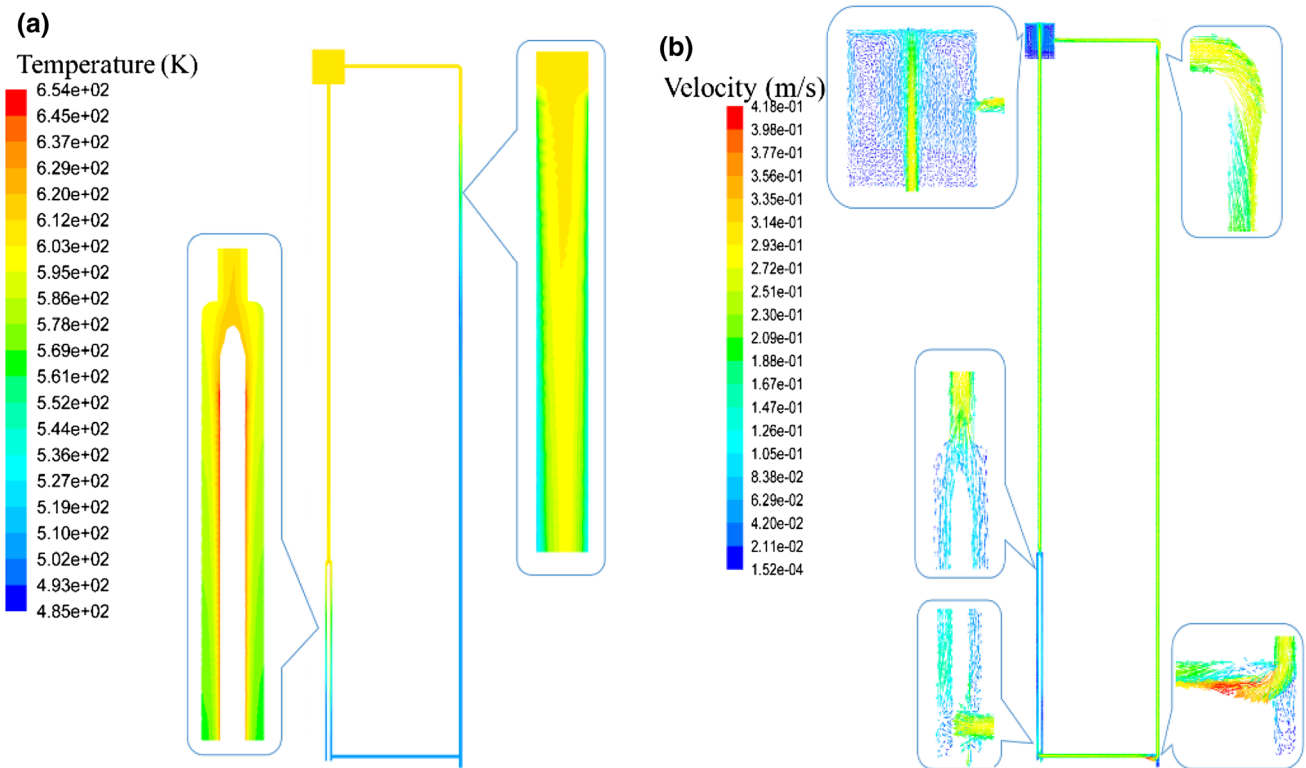


Fig. 3 CFD results at input power of 17.9 kW

## 5 Results and discussion

### 5.1 Experimental results and discussion

To understand the LBE flow characteristics in natural circulation loop and evaluate the CFD results, steady-state experiments at different heating powers were performed in the KYLIN-II TH natural circulation loop. At the first stage, flow rate of the loop was obtained by energy balance method. The power and temperatures at the inlet and outlet of the HS and HX were recorded. According to the conservation equation of energy, the mass flow rate was estimated from the input power and the temperature difference between the outlet and inlet of the HS.

Figure 4a shows the inlet and outlet temperature of the HS and the temperature difference at 17.9 kW input power, while Fig. 4b, c shows the temperature differences and LBE mass flow rate at different input powers, respectively. To investigate how the power impacts on natural circulation, the oil flow rate in the secondary loop was kept at the same conditions. Temperature in the primary loop increased continuously. Due to the LBE flow rate onset, the temperature differences increased to their maximum and then, as the flow started, decreased toward a stable value. After a transient of about 4 min, the temperature differences and mass flow rates stabilized, indicating the establishment of natural circulation. Also, it can be seen that the greater is the power, the higher is the temperature peak and the shorter is the transient time.

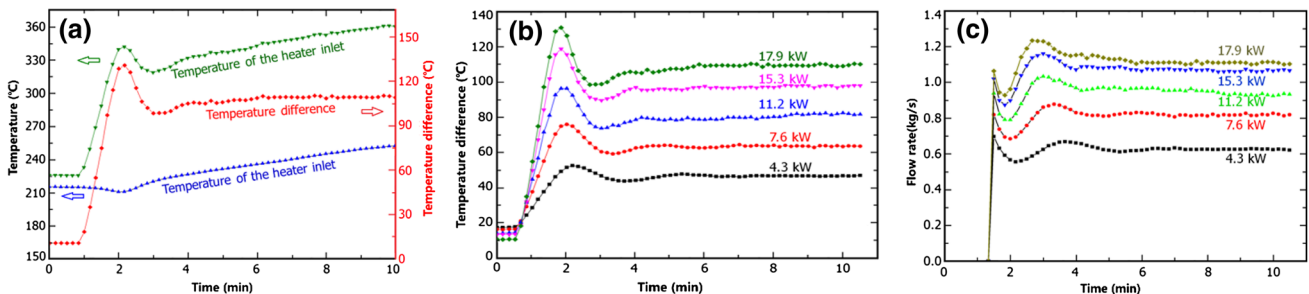
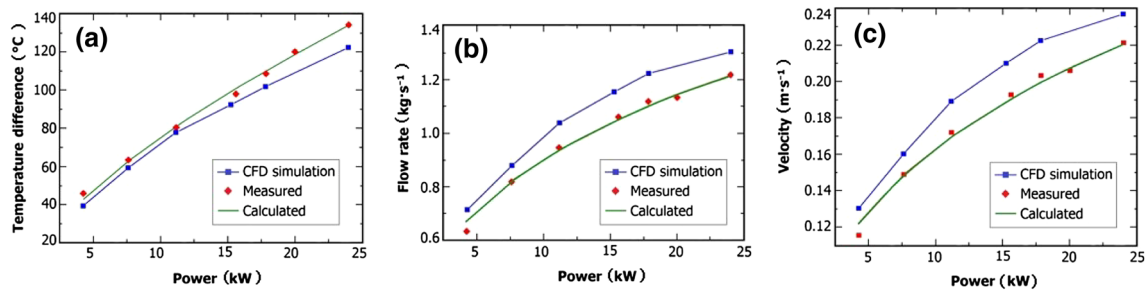


Fig. 4 Temperatures of the heater inlet and outlet at input power 17.9 kW (a) and the temperature differences and flow rates at different powers (b, c)



**Fig. 5** Comparison of theoretical, experimental and CFD results

## 5.2 Comparison of the results

The comparison of experimental and CFD results is shown in Fig. 5, where the temperature difference between the HS outlet and inlet, the mass flow rate and the average velocity vary with the input power. Owing to the property of large thermal expansion coefficient, the temperature difference could cause a difference in density between the hot leg and the cold leg. The density difference could introduce buoyancy force, which drives the LBE circulation in the loop. As a result, the temperature difference, mass flow rate and average velocity increase with the input power. At 17.9 kW, by the theoretical analysis, measurement and CFD simulation, the temperature differences between the outlet and inlet of HS are 110.3, 108.6 and 101.5 °C, respectively; the mass flow rates are 1.10, 1.12 and 1.20 kg s<sup>-1</sup>, respectively; and the average velocities are 0.200, 0.203 and 0.222 m s<sup>-1</sup>, respectively.

After optimization of the resistance coefficients, the theoretical analysis results agree well with the experimental results. However, the CFD simulation results deviate greatly from the experimental results. This may have two reasons:

- 1) Adiabatic condition is assumed in CFD. The inlet temperature of HS is experimentally lower than the outlet temperature of HX because of the heat losses, and the evaluated temperature difference is smaller than the experimental results.
- 2) The valve on the horizontal branch is not simulated in CFD model, hence an underestimation of the pressure drop and thus a larger mass flow rate.

## 6 Summary

Theoretical analysis was performed for the natural circulation and thermal-hydraulic performance in the KYLIN-II TH natural circulation loop to investigate the LBE flow characteristics. Steady-state experiments were performed at heating powers from 4.3 to 24.0 kW. A CFD simulation

with FLUENT code was carried out to predict the temperature and flow distribution in the loop. The natural circulation was easily established and stabilized in a few minutes. The theoretical analysis results of temperature differences, mass flow rate and velocity results agreed well with the experimental results, but the CFD prediction results had a maximum difference of 10% from the experimental data.

For further analysis of thermal-hydraulic performance in natural circulation of the LBE, experiments on transient state and heat transfer of natural circulation will be carried out. Gas enhanced circulation study is to be carried out, too.

**Acknowledgements** The authors would like to acknowledge the help from other members of FDS team in the experiment.

## References

1. OECD/NEA: Handbook on lead–bismuth eutectic alloy and lead properties, materials compatibility, thermal-hydraulics and technologies. OECD/NEA No. 6197. 2007 Edition. ISBN 978-92-64-99002-9, 15–26
2. Y.C. Wu, Y.Q. Bai, Y. Song et al., Conceptual design of china lead-based research reactor CLEAR-I. Nucl. Sci. Eng. **34**(2), 201–208 (2014). (in Chinese)
3. A. Stanculescu, IAEA activities in the area of partitioning and transmutation. Nucl. Instr. Methods Phys. Res. Sect. A **562**(2), 614–617 (2006). doi:10.1016/j.nima.2006.02.045
4. X. Cheng, J.E. Cahalan, P.J. Finch, Safety analysis of an accelerator driven test facility. Nucl. Eng. Des. **229**, 289–306 (2004). doi:10.1016/j.nucengdes.2004.01.003
5. A. Alemberti, V. Smirnov, C.F. Smith et al., Overview of lead-cooled fast reactor activities. Prog. Nucl. Energy (2013). doi:10.1016/j.pnucene.2013.11.011
6. C.F. Smith, W.G. Halsey, N.W. Brown et al., SSTAR: the US lead-cooled fast reactor (LFR). J. Nucl. Mater. **376**(3), 255–259 (2008). doi:10.1016/j.jnucmat.2008.02.049
7. C.B. Davis, Thermal-hydraulic analyses of transients in an actinide-burner reactor cooled by forced convection of lead–bismuth. Nucl. Eng. Des. **224**(2), 149–160 (2003). doi:10.1016/S0029-5493(03)00104-3
8. W. Ma, E. Bubelis, A. Karbojian et al., Transient experiments from the thermal-hydraulic ADS lead bismuth loop (TALL) and comparative TRAC/AAA analysis. Nucl. Eng. Des. **236**(13), 1422–1444 (2006). doi:10.1016/j.nucengdes.2006.01.006

9. W. Ma, A. Karbojian, B.R. Sehgal, Experimental study on natural circulation and its stability in a heavy liquid metal loop. *Nucl. Eng. Des.* **237**, 1838–1847 (2007). doi:[10.1016/j.nucengdes.2007.02.023](https://doi.org/10.1016/j.nucengdes.2007.02.023)
10. M. Tarantino, S. De Grandis, G. Benamati et al., Natural circulation in a liquid metal one-dimensional loop. *J. Nucl. Mater.* **376**(3), 409–414 (2008). doi:[10.1016/j.jnucmat.2008.02.080](https://doi.org/10.1016/j.jnucmat.2008.02.080)
11. A. Borgohain, B.K. Jaiswal, N.K. Maheshwari et al., Natural circulation studies in a lead bismuth eutectic loop. *Prog. Nucl. Energy* **53**(4), 308–319 (2011). doi:[10.1016/j.pnucene.2010.10.004](https://doi.org/10.1016/j.pnucene.2010.10.004)
12. Y.C. Wu, Q.Y. Huang, Z.Q. Zhu et al., Progress in design and development of series liquid lithium-lead experimental loops in China. *Nucl. Sci. Eng.* **29**(2), 161–169 (2009). (in Chinese)
13. Y.C. Wu, F.D.S. Team, Conceptual design activities of FDS series fusion power plants in China. *Fusion Eng. Des.* **81**(23–24), 2713–2718 (2006). doi:[10.1016/j.fusengdes.2006.07.068](https://doi.org/10.1016/j.fusengdes.2006.07.068)
14. Y.C. Wu, F.D.S. Team, Conceptual design of the China fusion power plant FDS-II. *Fusion Eng. Des.* **83**(10–12), 1683–1689 (2008). doi:[10.1016/j.fusengdes.2008.06.048](https://doi.org/10.1016/j.fusengdes.2008.06.048)
15. Y.C. Wu, J.Q. Jiang, M.H. Wang et al., A fusion-driven sub-critical system concept based on viable technologies. *Nucl. Fusion* **51**(10), 103036 (2011). doi:[10.1088/0029-5515/51/10/103036](https://doi.org/10.1088/0029-5515/51/10/103036)
16. Y.C. Wu, Design status and development strategy of China liquid lithium–lead blankets and related material technology. *J. Nucl. Mater.* **367–370**, 1410–1415 (2007). doi:[10.1016/j.jnucmat.2007.04-031](https://doi.org/10.1016/j.jnucmat.2007.04-031)
17. Y.C. Wu, F.D.S. Team, Conceptual design and testing strategy of a dual functional lithium–lead test blanket module in ITER and EAST. *Nucl. Fusion* **47**(11), 1533–1539 (2007). doi:[10.1088/0029-5515/47/11/015](https://doi.org/10.1088/0029-5515/47/11/015)
18. Y.C. Wu, F.D.S. Team, Fusion-based hydrogen production reactor and its material selection. *J. Nucl. Mater.* **386–388**, 122–126 (2009). doi:[10.1016/j.jnucmat.2008.12.075](https://doi.org/10.1016/j.jnucmat.2008.12.075)
19. Y.C. Wu, J.P. Qian, J.N. Yu, The fusion-driven hybrid system and its material selection. *J. Nucl. Mater.* **307–311**, 1629–1636 (2002). doi:[10.1016/S0022-3115\(02\)01272-2](https://doi.org/10.1016/S0022-3115(02)01272-2)
20. Q.Y. Huang, C.J. Li, Y. Li et al., Progress in development of China low activation martensitic steel for fusion application. *J. Nucl. Mater.* **367–370**, 142–146 (2007). doi:[10.1016/j.jnucmat.2007.03.153](https://doi.org/10.1016/j.jnucmat.2007.03.153)
21. J.H. Choa, A. Batta, V. Casamassima et al., Benchmarking of thermal hydraulic loop models for Lead-Alloy Cooled Advanced Nuclear Energy System (LACANES), Phase-I: isothermal steady state forced convection. *J. Nucl. Mater.* **415**, 404–414 (2011). doi:[10.1016/j.jnucmat.2011.04.043](https://doi.org/10.1016/j.jnucmat.2011.04.043)